Multi-scale simulation of the 1,3-butadiene extraction separation process with an ionic liquid additive

Xiao Tian,[a,b] Xiangping Zhang,*[a] Lu Wei,[a] Shaojuan Zeng,[a] Lei Huang[a] and Suojiang Zhang*[a]

Received 15th September 2009, Accepted 19th May 2010
First published as an Advance Article on the web 14th June 2010
DOI: 10.1039/b918924f

A multi-scale simulation method is proposed to enable screening of ionic liquids (ILs) as entrainers in extractive distillation. The 1,3-butadiene production process with acetonitrile (ACN) was chosen as a research case to validate the feasibility of the methodology. *Ab initio* calculations were first carried out to further understand the influence of ionic liquids on the selectivity of ACN and the solubility of C_4 fractions in $[C_nMIM][PF_6](n = 2–8)$, $[C_2MIM][X]$ ($X = BF_4^-$, Cl^-, PF_6^-, Br^-), by investigating the microstructure and intermolecular interaction in the mixture of C_4 fractions and several selected ionic liquids. It was found that the selectivity of the ionic liquid is determined by both its polarity and hydrogen-bonding ability. Based on the analysis, a suitable ionic liquid was chosen. With the *ab initio* calculation, *a priori* prediction of thermophysical data of the IL-containing system was performed with COSMO-RS. The calculation revealed that the selectivity of the extractive solvent was increased by an average of 3.64% after adding $[C_2MIM][PF_6]$. With above calculations, an improved ACN extraction distillation process using ILs as an entrainer was proposed, and a configuration for the new process was constructed. Based on the established thermodynamic models which have considered the properties from the molecular structure of ILs, process simulation was performed to obtain the process parameters which are important for the new process design. The simulation results indicated that the temperatures at the bottom of the extractive distillation column with the ionic liquid as an additive are lowered by an average of 3.1 °C, which is significant for inhibition of polymerization. We show that the ACN consumption using this process can be lowered by 24%, and the energy consumption can likewise be lowered by 6.62%.

1. Introduction

1,3-Butadiene (1,3-BD), which is an important petrochemical base material and mainly used to produce synthetic rubber,[1–3] is principally produced by extractive distillation. Acetonitrile (ACN) is one of the three most widely used selective solvents to extract 1,3-BD from C_4 hydrocarbon mixtures.[4–7] However, the relatively large amount of recycled ACN and high solvent/feed mass ratio (up to 8) in the current commercial ACN process leads to greater consumption of energy, and also a rather high temperature at the bottom of the extractive distillation column,[8]which is the major cause of polymerization. Additionally, the basic solvent ACN is easily hydrolyzed to acetic acid and ammonia,[9–11] which causes relatively high levels of corrosion. It has been reported that adding a third component (such as organic compounds and salts) to the traditional ACN solvent can decrease the distillation temperature and reduce the dosage of ACN.[8,12] Compared with organic compounds, salts are more effective as additives in increasing the relative volatility of C_4 at infinite dilution, according to Zhigang Lei *et al.*[8] However, conventional salt-added extractive distillation has several inherent shortcomings, such as difficulty in recycling of the salt and likelihood of the pipeline becoming jammed.[13]

Fortunately, room-temperature ionic liquids (RTILs), which are fused salts composed of large asymmetric organic cations and inorganic or organic anions, have the advantages of both liquid solvents and solid salts.[14] Among the numerous RTILs, ILs based on imidazolium cations have been proven to be highly attractive and versatile[15] on account of their favorable characteristics, *e.g.*, moisture- and air-stability, easy recycling and being a good solvent for a wider variety of organic and inorganic chemical compounds.[16–18] In addition, imidazolium ILs are "designable" because structural modifications in both the cation (especially the 1- and 3-positions of the imidazolium ring) and anion permit the tuning of properties, *e.g.*, miscibility with water and organic solvents, melting point and viscosity.[19] Consequently, imidazolium ILs hold much potential for applications in the field of separation.[17,20,21]

However, the tremendous number of possible imidazolium ILs pose a challenge, namely to identify a suitable ionic liquid for a given separation process. Conquering this challenge through experiment is possible but so time-consuming as to be hardly feasible. Compared with experimental methods, computer

[a]*State Key Lab of Multi-phase Complex Systems, Institute of Process Engineering, Chinese Academy of Sciences, Beijing, 100190, China. E-mail: sjzhang@home.ipe.ac.cn, xpzhang@home.ipe.ac.cn; Fax: +86-10-82627080; Tel: +86-10-82627080*
[b]*Graduate University of Chinese Academy of Sciences, 100049, Beijing, China*

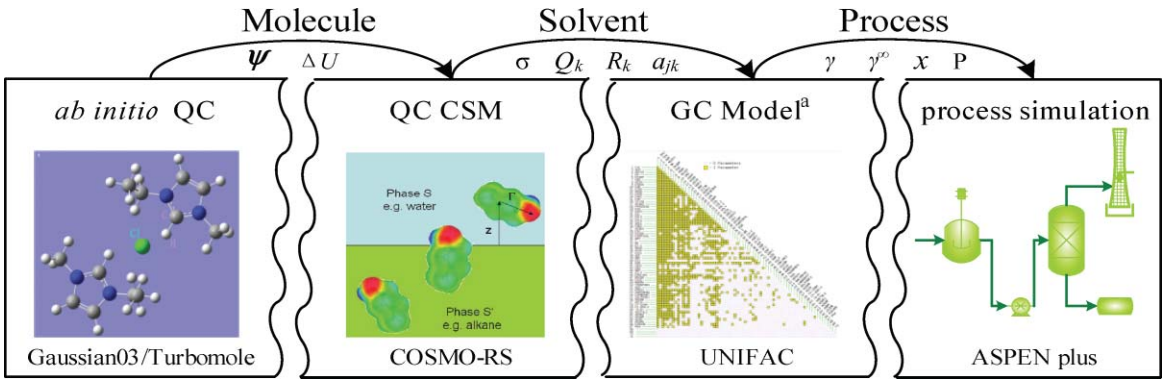

Fig. 1 Schematic diagram of the methodology described in this paper. [a] From http://commons.wikimedia.org/wiki/File:UNIFAC_Parameter_Matrix_Consortium_2008.png.

simulations are time-saving and eco-friendly, and have been employed to screen and design a desired ionic liquid with excellent performance.[22]

In this study, the multi-scale simulation methodology illustrated in Fig. 1 is proposed for identifying a suitable IL for a separation process. Quantum-chemical (QC) simulations are first carried out to investigate the relationship between the structure and the properties of ILs, and to determine what the key factors are that will improve the absorbency and selectivity of the ionic liquids. Then, *a priori* prediction is employed to obtain thermodynamic data of the IL-containing system including activity coefficients, equilibrium vapor pressures and Henry constants with a QC continuum solvation model (CSM), COSMO-RS[23] (Conductor-like Screening Model for Realistic Solvents). To predict the thermodynamic data of the novel system over a wide range of concentration and temperature, the group interaction parameters in UNIFAC model are fitted to data from COSMO-RS. Then with these parameters, process simulation was completed with a commercial simulator, Aspen Plus, which is widely used in the chemical engineering field.[24–27]

2. Computational methodology

2.1 *Ab initio* calculations

All the calculations were performed with GAUSSIAN03.[28] *Ab initio* DFT using the well-established Becke three-parameter hybrid functional[29] with the correlation functional of Lee, Yang and Parr[30] (B3LYP) was used, combined with 6-31G* basis set, of which the abilities to calculate the structure and energy of ILs ion pair have been widely demonstrated. Each optimized structure was checked to be a true minimum and not a saddle point by calculation.

2.2 Thermodynamic calculation

All the thermodynamic properties of the IL-containing system, including equilibrium vapor pressures and activity coefficients of the solute molecules, were predicted by COSMOtherm,[31–33] a useful prediction method for thermodynamic equilibria of fluids and liquid mixtures. All the input files of COSMOtherm were produced by using the COSMO model from TURBOMOLE 5.10[34,35] at the RI-DFT/BP86/TZVP level.

2.3 Process simulation

With the thermodynamic properties obtained from the calculations above, Aspen Plus software was used to simulate the proposed ACN interactions with ionic liquid. The UNIFAC model was chosen as a global thermodynamic model, and the IDEAL model was employed in the ordinary distillation section. The rigorous multistage separation (RADFRAC) model was adopted to calculate the distillation columns in the process.

3. Results and discussion

3.1 *Ab initio* calculations

Since the main interest of this work lies in the interaction energy, detailed geometry optimization procedures for the ILs, ACN and C_4 fractions are not presented, and only the most stable structures are shown in the interaction energy analysis.

3.1.1 The mechanism of separation of C_4 fractions using acetonitrile and water. With the aim of component separation, polarity is one of the most important properties of the selective solvent. A semi-empirical theory of solution thermodynamics, revealing which factors are related to the separation ability of a solvent, was established by Prausnitz *et al.*[36] The theory can be illustrated by eqn (1):

$$RT\ln S_{23} = [\delta_1^{p2}(V_2 - V_3)] + [V_2(\delta_1^{n} - \delta_2)^2 - V_3(\delta_1^{n} - \delta_3)^2] + [2V_3\xi_{13} - 2V_2\xi_{12}] \quad (1)$$

where subscripts 1–3 represent entrainers, the light component and the heavy component to be separated; superscripts n and p refer to nonpolar and polar; V is the molar volume; δ is Hansen's solubility parameter and ξ is the indication energy per unit volume. In eqn (1), the first term representing the effect of the polarity was considered as the main contributor to the selectivity of a component by Prausnitz.

Since molecular sizes of C_4 fractions are very close to each other, as shown in Fig. 2, it is difficult to separate them unless extractive distillation is used. In the traditional ACN process – one of the three most widely used extractive distillation processes to produce 1,3-BD – the extractive solvent consists of two components: ACN and water. Their polarities obtained from *ab initio* calculations are listed in Table 1. It can be seen that the dipole of water (2.09 Debye) is rather less than that of ACN

Table 1 Dipoles, molar volumes, molecular radii and interaction energies with 1,3-butadiene of all entrainers (calculated at the B3LYP 6-31G* level)

Name	Dipole (Debye)	V (cm^3 mol^{-1})	r (Å)	ΔU^a (kJ mol^{-1})
Water	2.090	15.06	2.50	12.96
Acetonitrile	3.810	37.95	3.22	8.340
[C_2MIM][BF_4]	11.97	108.7	4.36	28.50
[C_2MIM][Cl]	12.45	124.0	4.53	25.87
[C_2MIM][Br]	12.61	112.0	4.40	38.84
[C_2MIM][PF_6]	14.10	112.5	4.40	29.63
[C_3MIM][PF_6]	13.62	141.4	4.71	25.49
[C_4MIM][PF_6]	13.31	146.8	4.76	25.18
[C_5MIM][PF_6]	13.25	149.9	4.80	25.02
[C_6MIM][PF_6]	13.23	153.8	4.83	25.12
[C_7MIM][PF_6]	13.95	201.0	5.24	29.56
[C_8MIM][PF_6]	13.96	251.2	5.60	32.18
[C_2(OH)MIM][PF_6]	13.34	146.0	4.76	24.24
[C_2(OMe)MIM][PF_6]	12.80	153.3	4.83	24.99
[$C_2(NH_2)$MIM][PF_6]	13.21	148.5	4.78	26.77
1-Ethoxy-2-propanol	2.344	86.17	4.07	14.71
Glycol	0.002	32.29	3.07	12.78

^{a} ΔU (kJ mol^{-1}) = $U_{\text{entrainer}+1,3\text{-butadiene}} - U_{\text{entrainer}} - U_{1,3\text{-butadiene}}$.

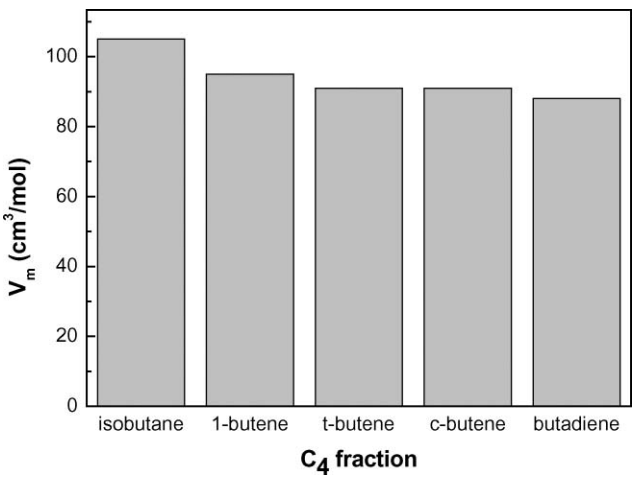

Fig. 2 Molar volume of C_4 fractions.

(3.81 Debye), implying a lower polarity for water. So, based on eqn (1), the presence of water should weaken the selectivity of ACN. However, in practice, water is a major additive to enhance the selectivity of the extractive solvent in the traditional ACN processes.[37] This inconsistency implies that some other term that plays a key role in determining the selectivity of a solvent should be included in eqn (1).

In this study, energy analysis, which is often used to investigate physical properties of components such as selectivity and melting point,[38–44] was carried out to investigate the extraction mechanism of the solvent. Fig. 3 shows the most stable configurations of water and ACN with 1,3-BD. Interaction energies between the components and 1,3-BD were calculated and are listed in Table 1. As shown, water has a stronger interaction with 1,3-BD than ACN, although the latter has a larger polarity. In the configuration 3a, the distances N···H1 (2.97 Å) and N···H2 (3.00 Å) are larger than the sum of van der Waals radii of the relevant atoms (2.75 Å), as shown in Table 2, indicating that no hydrogen bonding occurs between the two molecules. In

Table 2 Van der Waals radii r_w (nm) of the elements involved[55]

	H	C	O	P	Br	F	N	Cl
r_w	1.20	1.70	1.52	1.80	1.95^a	1.47	1.55	1.75

^{a} Van der Waals radius as given by Pauling.

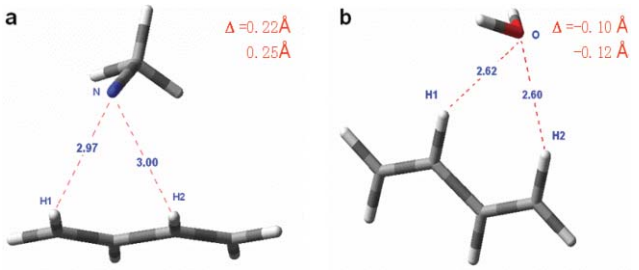

Fig. 3 The most stable configurations for 1,3-butadiene and (a) acetonitrile, and (b) water (calculated at the B3LYP 6-31G* level). Hydrogen bonds are indicated with dotted lines, and the distances are in Å.

the configuration 3b, however, the distances O···H1 (2.62 Å) and O···H2 (2.60 Å) are much less than the sum of the van der Waals radii (2.72 Å). In addition, the angles ∠O···H1–C and O···H2–C are 152° and 150°, respectively. This data indicate that two strong hydrogen bonds (HBs) are involved in the configuration b. Consequently, it could be inferred that hydrogen bonding is the key factor determining the strong interaction between water and 1,3-BD, and that a term for hydrogen bonding (HB) should be added to eqn (1). To express the strength of HB, two parameters, θ and Δ, were used in this work. θ refers to the angle of HB, while Δ represents the difference between the length of HB and the sum of the van der Waals radii of the relevant atom. Consequently, eqn (1) was modified to eqn (2):

$$RT \ln S_{23} = P + D + I + H \quad (2)$$

where $P = \delta_1^{p2}(V_2 - V_3)$, $D = V_2(\delta_1^n - \delta_2)^2 - V_3(\delta_1^n - \delta_3)^2$, $I = 2V_3\xi_{13} - 2V_2\xi_{12}$, and $H = H(\Delta,\theta)$, representing the polar effect, the dispersion effect, the inductive effect and the HB effect, respectively.

According to eqn (2), a suitable additive should possess three characteristics: strong hydrogen-bonding ability, large polarity and small molecular size. It was reported that hydrogen bonds are present in the bulk of room-temperature ionic liquids, which must be strongly polar in order to be liquid salts. In addition, hydrogen-bonded networks have been proven to occur in imidazolium ILs by both experimental measurements and computer modeling.[45–47] Therefore, we hypothesized that imidazolium should have good performance in enhancing the selectivity of ACN for C_4 fractions. This point will be proven in the following section.

3.1.2 Influence of ILs on the interaction energy between ACN and C_4 fractions. In this section, the effect of imidazolium ionic liquids on the selectivity of ACN was investigated using the energy analysis method. Fig. 4a shows interaction energies between ACN and typical C_4 fractions, *viz.*, 1,3-BD, *cis*-butene, *trans*-butene, isobutene and *n*-butane. As shown in the figure, the interaction energy between ACN and 1,3-BD is largest,

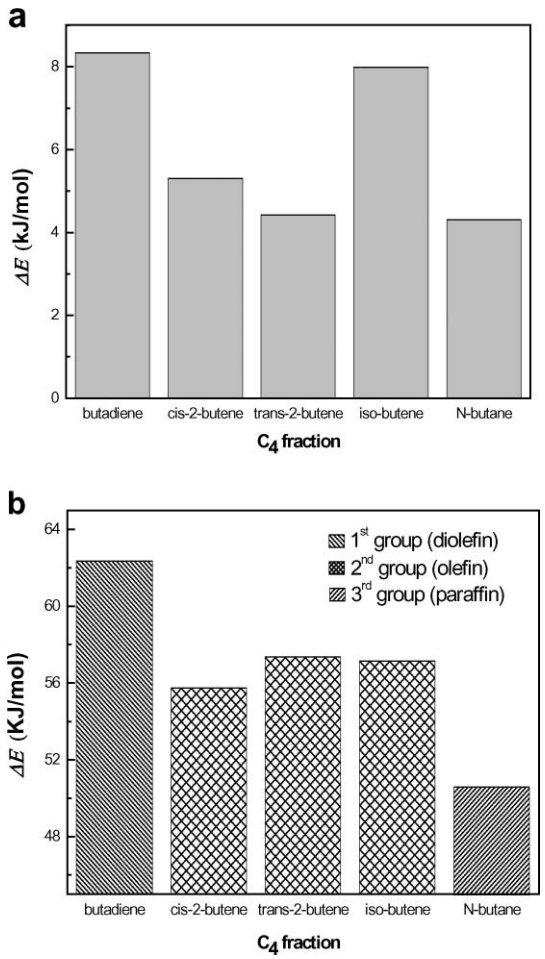

Fig. 4 Interaction energy between ACN and C_4 fraction (a) without and (b) with $[C_2MIM][PF_6]$.

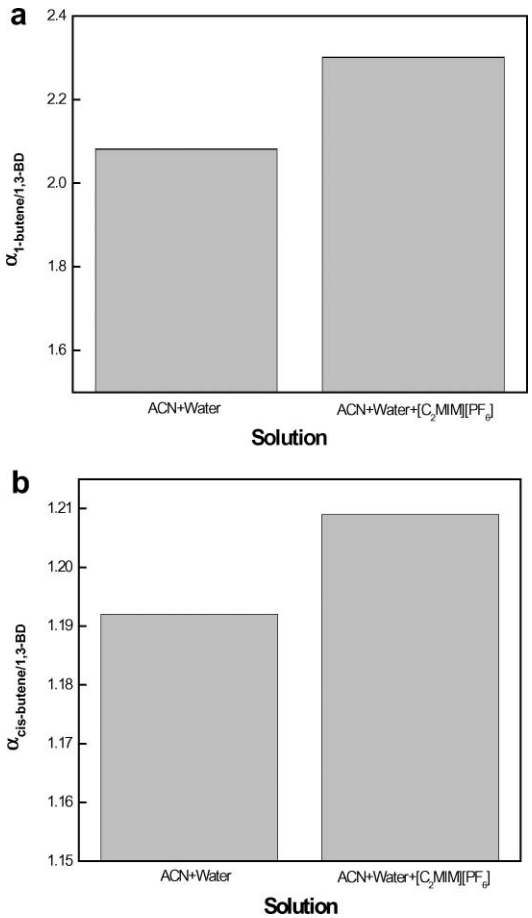

Fig. 5 Influence of $[C_2MIM][PF_6]$ on the volatility of (a) 1-butene and (b) *cis*-butene relative to 1,3-butadiene.

implying that 1,3-BD is the heaviest component among the C_4 fractions in the extractive distillation. The figure also shows small differences between the interaction energies, *e.g.*, the value between 1,3-BD and isobutene is only 0.3 kJ mol^{-1}, which means separating the two components is difficult without any additive. As a comparison, Fig. 4b presents the interaction energies in the presence of $[C_2MIM][PF_6]$, which is a typical imidazolium ionic liquid. An interesting phenomenon should be noted in Fig. 4b, namely, that three distinct groups in term of interaction energy emerge after adding the ionic liquid. Specifically, 1,3-BD belongs to the first group, with an interaction energy above 58 kJ mol^{-1}; alkenes belong to the second group, with interaction energies between 54 and 58 kJ mol^{-1}; and *n*-butane, as an alkane, belongs to the last group, with an interaction energy below 54 kJ mol^{-1}. Consequently, it could be concluded the imidazolium IL improves drastically the selectivity of ACN. In addition, comparison of Fig. 4a and 4b also reveals that in the presence of ionic liquid the average interaction energy increases from 6.1 kJ mol^{-1} to 56.7 kJ mol^{-1}, indicating the solubility of the C_4 fractions in the solvent mixture will increase significantly.

To further investigate the effect of ILs on selectivity of the extractive solvent, the relative volatilities of 1-butene and *cis*-butene to 1,3-BD, $\alpha_{1\text{-butene/1,3-BD}}$ and $\alpha_{cis\text{-butene/1,3-BD}}$, were measured at 303 K, as shown in Fig. 5a and b. It was found that the relative volatilities clearly increase in the presence of $[C_2MIM][PF_6]$, indicating the selectivity of the extractive solvent has been improved. These experimental findings also demonstrate that the above theoretical conclusion based on energy analysis is reasonable and reliable.

Why should an IL improve the performance of ACN? The reason lies in the unique properties of ILs – strong hydrogen-bonding ability and high polarity. Fig. 6 reveals that two moderate HBs occur between $[C_2MIM][PF_6]$ and 1,3-BD with Δ values of –0.26 Å and –0.24 Å, respectively. In addition, the dipole of $[C_2MIM][PF_6]$ is about four times as large as that of ACN, as shown in Table 1.

3.1.3 Selection of a suitable IL using *ab initio* calculations. As demonstrated in the previous section, the selectivity and dissolving capacity of the extractive solvent can be improved by addition of imidazolium ILs. However, the structure of an imidazolium IL has a significant influence on its polarity, hydrogen bonding ability and molecular size, which are key properties for its separation application.

Screening of anions. In view of the availability and stability, four types of anions were investigated including Br^-, Cl^-, BF_4^- and PF_6^-. Fig. 7 shows the change of the interaction energy between ILs containing the cation $[C_2MIM]^+$ and 1,3-BD. The bromide salt has the largest interaction energy (38.84 kJ mol^{-1}), while the hexafluorophosphate takes second

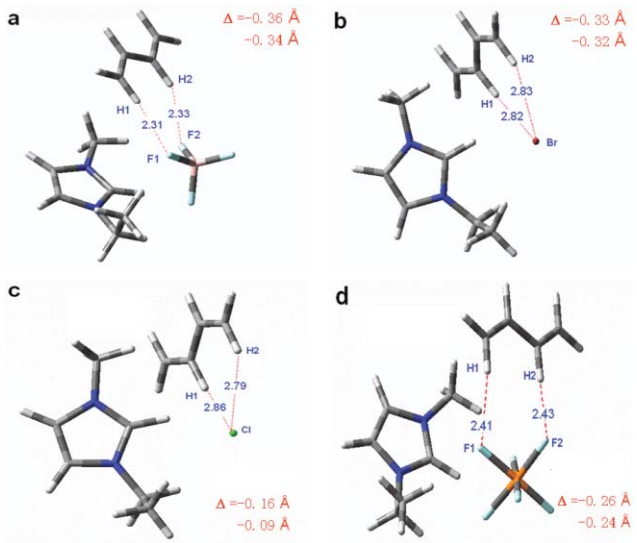

Fig. 6 Stable configurations for 1,3-butadiene and (a) [C_2MIM][BF_4], (b) [C_2MIM][Br], (c) [C_2MIM][Cl], and (d) [C_2MIM][PF_6] (calculated at the B3LYP 6-31G* level). Hydrogen bonds are indicated with dotted lines, and the distances are in Å.

place (29.63 kJ mol^{-1}). However, our experimental work shows that ILs with anion Br^- are strongly corrosive materials, which would damage the equipment. In contrast, the hexafluorophosphates are rather less corrosive. Thus, it was concluded that imidazolium ILs containing PF_6^- would be more best for our ACN process.

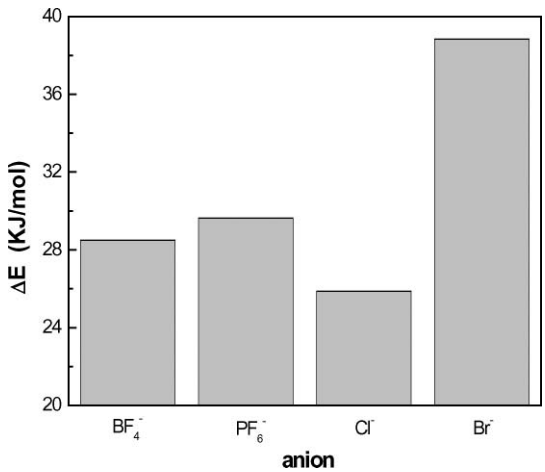

Fig. 7 Interaction energy between 1,3-butadiene and [C_2MIM][X] (X = BF_4^-, PF_6^-, Cl^-, Br^-).

To explain this conclusion, the most stable configurations of the ILs and butadiene were calculated at the B3LYP 6-31G* level. As shown in Fig. 6, two HBs are formed between ILs and butadiene in each configuration, and the ILs can be arranged in order of hydrogen-bonding ability as [C_2MIM][BF_4] > [C_2MIM][Br] > [C_2MIM][PF_6] > [C_2MIM][Cl]. Although [C_2MIM][BF_4] has the strongest hydrogen-bonding ability, with Δ –0.36 Å and –0.34 Å, its dipole (11.97 Debye) is significantly smaller than that of [C_2MIM]Br (12.61 Debye) and [C_2MIM][PF_6] (14.10 Debye), and therefore has smaller interaction energy than these latter two ILs.

In addition, Fig. 6 also indicates that 1,3-BD strongly organizes around anions through a hydrogen-bonding interaction, implying that the hydrogen-bonding ability of the ionic liquid mainly depends on the structure of the anion, and is dependent only slightly on the cation. To understand its mechanism, the electron density of [C_2MIM][PF_6] as an example was investigated. As shown in Fig. 8, the most charge-negative sites in [C_2MIM][PF_6] include the F atoms on the anion and the N atoms on the imidazole ring. The regions around these sites can be considered for potential interactions with 1,3-BD. However, the regions on two N atoms are unfavorable for HB formation due to the shielding effect resulting from the alkyl side chains. Therefore, a reasonable conjecture was made that the performance of ILs with the same anions should rest in their polarity and molecular size, which will be further verified in the next section.

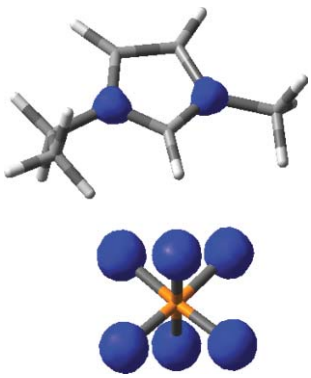

Fig. 8 Electron density of [C_2MIM][PF_6] (isoval = 0.45, mapped with total density).

Screening of cations. Fig. 9 shows the effect of the length of alkyl side chain in the imidazolium cation on the interaction energy between ILs and 1,3-BD. As shown in Fig. 9, the interaction energy first decreases and then begins to increase as *n* becomes larger than 6. As was explained in Section 3.1.2, the interaction energy between solutes and solvents could reflect the relative volatility of the former and the selectivity of the later. To strengthen this conclusion, relative volatilities of *cis*-butene and

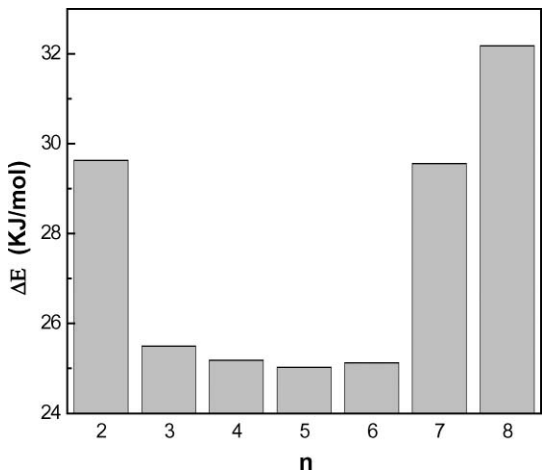

Fig. 9 Interaction energy between 1,3-butadiene and [C_nMIM][PF_6] (n = 2–8).

1,3-butadiene in [C_nMIM][PF_6] (n = 2, 4, 6, 8) were measured at 303 K, as shown in Fig. 10, indicating that the length of alkyl side chain has the same influence on both the interaction energy and the relative volatility. With regard to the influence of the length of the alkyl side chain, this lies in the structural characteristics of the ILs. It can be seen from Table 1 that the dipoles of the ILs have almost the same trend as the interaction energy as n increases. The phenomenon suggests that, for ILs with a given anion, the interaction energy mainly depends on the dipole of the IL. On the other hand, the inductive effect should be considered with the increase in molecular sizes of ILs. Just as shown in Table 1, the interaction energy of [C_8MIM][PF_6] is stronger than that of [C_2MIM][PF_6] by 3.55 kJ mol^{-1}, although the later has a larger dipole.

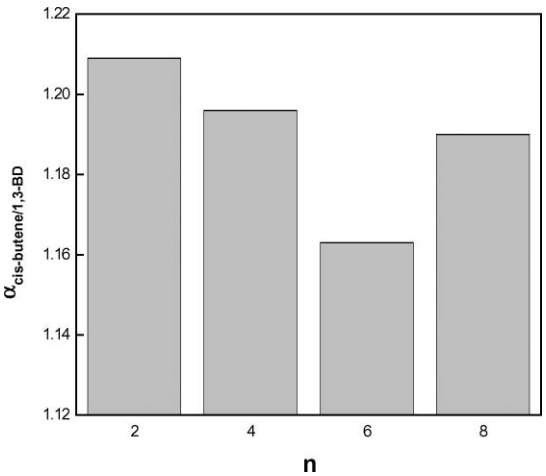

Fig. 10 Influence of the length of alkyl side chain on the relative volatility of *cis*-butene to 1,3-butadiene.

The effect of substituent groups on the alkyl side chain on the interaction energy was also considered. Three functional groups were studied, *viz.*, NH_2, OMe and OH, which were reported to be effective at enhancing the polarity of ILs.[48,49] However, Fig. 11 indicates that the interaction energy decreases after introducing these groups. This is mainly because they decrease the polarity of IL, as showed in Table 1. This shows that adding the functional groups would be unfavorable for increasing the selectivity of the IL.

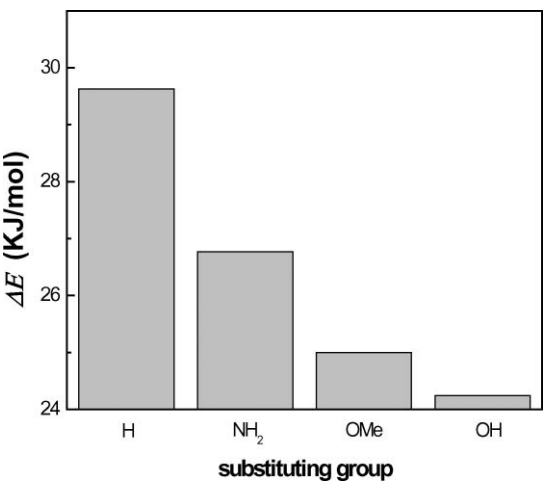

Fig. 11 Interaction energy between 1,3-butadiene and [C_2(R)MIM][PF_6] (R = H, NH_2, OMe, OH).

Table 3 Equilibrium vapor composition of additive (wt%, at 0.35 MPa) using different extractive solvents

	Solvent mixture		
Additive	ACN–water 90 : 10	ACN–water–EP 77.5 : 15 : 7.5	ACN–water–[C_2MIM][PF_6] 77.5 : 15 : 7.5
Isobutane	4.533	3.654	4.603
1-Butene	45.70	46.37	45.85
1,3-Butadiene	33.58	34.44	30.45
trans-Butene	3.868	3.563	3.750
cis-Butene	2.537	2.412	2.410

Consequently, [C_2MIM][PF_6], which possesses strong hydrogen-bonding ability, large polarity, small molecular volume and unbranched group, was determined as a suitable ionic liquid for separating C_4 fractions.

3.1.4 Comparison of the chosen ionic liquid ([C_2MIM][PF_6]) with reported additives. To assess the performance of the chosen ionic liquid, a comparison was made with two reported additives: glycol and 1-ethoxy-2-propanol.[50] As shown in Fig. 12 and Fig. 13, both of the reported additives are inferior to [C_2MIM][PF_6] in terms of hydrogen-bonding ability and interaction energy with 1,3-BD – that is, [C_2MIM][PF_6] is the most efficient in improving the selectivity of ACN. We also compared the calculation results with the experimental results, as shown in Table 3. It should be noted that weight fractions of light components such as *cis*-butene increases most noticeably while using the IL-containing mixture as the extractive solvent under the same conditions, which means their relative volatilities are enhanced. The finding is in good agreement with the above theoretical prediction.

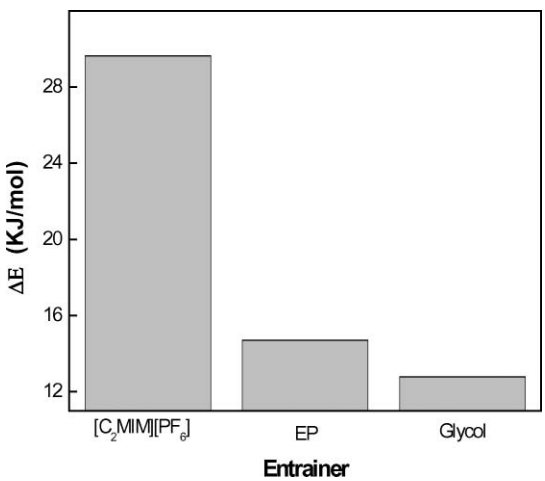

Fig. 12 Interaction energy between 1,3-butadiene and C (C = [C_2MIM][PF_6], EP, glycol).

3.2 Thermodynamic calculations

3.2.1 Selectivity analysis of IL-containing entrainer using COSMOtherm. Selectivity provides a useful criterion for selection of a suitable entrainer. For the IL-containing system

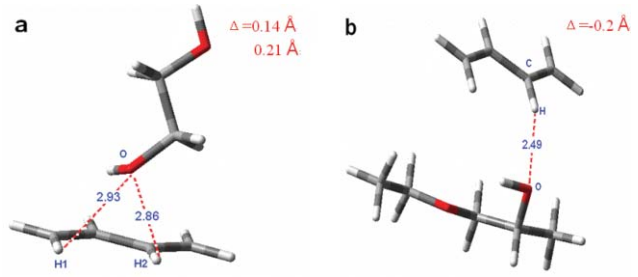

Fig. 13 Stable configurations for 1,3-butadiene and (a) glycol, (b) EP (calculated at the B3LYP 6-31G* level). Hydrogen bonds are indicated with dotted lines, and the distances are in Å.

discussion here, the vapor phase of which can be considered to be an ideal gas, the selectivity of the extractive solvent can be defined as eqn (3):where S is the selectivity of a solvent, α_{ij} is the

$$S_{ij} = \frac{\alpha_{ij}^{s}}{\alpha_{ij}} = \left(\frac{\gamma_i p_i^0}{\gamma_j p_j^0}\right)^{s} \times \frac{\gamma_j p_j^0}{\gamma_i p_i^0}$$
$$\alpha_{ij} = \frac{K_i}{K_j} = \frac{\gamma_i p_i^0}{\gamma_j p_j^0} \quad (3)$$

relative volatility of solute i to j; K_i, γ_i and p_i are the equilibrium constant, activity coefficient and equilibrium partial pressure of component i, respectively; superscript s represents the solvent, and superscript 0 means a pure component.

The COSMO-RS model can be used to evaluate the separation ability of ionic liquids,[51] and the calculation procedure has been described in the literature.[52] Table 4 shows the activity coefficients and vapor pressures of the solutes in entrainers, with and without IL, as calculated using the COSMO-RS model. Based on eqn (3), the selectivity of the two entrainers was compared, as shown in Table 5. It is found that the selectivity of the extractive solvent mixture increased by an average of 3.64% upon adding [C_2MIM][PF_6].

Table 4 Activity coefficients and equilibrium vapor pressures of the solutes with and without the IL [C_2MIM][PF_6]

Component	Activity coefficient		Equilibrium vapor pressure (kPa)
	No IL	IL	
ACN	1.027	0.992	6.990
1,3-Butadiene	2.849	3.195	388.7
trans-2-Butene	7.674	8.884	512.9
Water	3.604	5.173	1.348
cis-2-Butene	6.823	7.843	528.2
Isobutane	19.30	23.18	669.6
1-Butyne	1.576	1.789	134.0
Vinylacetylene	0.914	1.042	139.1
n-Butane	19.74	23.61	710.2
1-Butene	6.939	8.017	511.1

3.2.2 Calculation of UNIFAC group interaction parameters using COSMOtherm. Currently, it is a challenge to simulate an IL-containing process by current commercial process simulators, *e.g.*, Aspen Plus and PRO/II, because of the shortage of the experimental data of thermodynamic properties of pure ILs or their mixtures. In this work, group interaction parameters involving [C_2MIM][PF_6] in the UNIFAC model (chosen to be the global property method during the simulation), were regressed based on the data from COSMOtherm.

According to Wang *et al.*,[53] the UNIFAC model can describe and predict well the Vapor–Liquid Equilibrium (VLE) and Liquid–Liquid Equilibrium (LLE) of IL-containing mixtures. The UNIFAC model was proposed in 1975 by Fredenslund *et al.*,[54] in which the excess Gibbs free energy is made of two contributions: a combinatorial part and a residual part. Accordingly, the activity coefficient of a solvent i, γ_i, can be written as eqn (4):

$$\ln \gamma_i = \ln \gamma_i^{C} + \ln \gamma_i^{R} \quad (4)$$

where γ_i^{C} is the combinatorial contribution to activity coefficient accounting for the repulsive interaction due to the molecular size and shape, and γ_i^{R} is the residual activity coefficient arising from intermolecular forces represented by corresponding group interaction parameters (see ref. 55 for a detailed description of the original UNIFAC model).

In this study, UNIFAC interaction energy parameters between different groups were fitted to activity coefficient data from COSMOtherm calculations. The ionic liquid is 'decomposed' into two groups, [MMIM][PF_6] and CH_2, as shown in Fig. 14. For the new group [MMIM][PF_6], the volume and surface area parameters R and Q were calculated by summing up those of the constituent subgroups. All the related group parameters of R and Q are listed in Table 6.

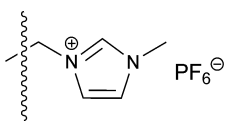

Fig. 14 'Decomposition' of ionic liquid [C_2MIM][PF_6] for the purposes of determining the interaction energy parameters.

On the basis of these group parameters and the binary parameters available in the literature, the new interaction parameters between [MMIM][PF_6] and other groups were fitted to the activity coefficient data of the 10 components in the ionic liquid. The values of the binary parameters were determined by minimizing the following objective function:

Table 5 Increase of the selectivity for the solutes after adding the ionic liquid

Component	*trans*-2-Butene	*cis*-2-Butene	Isobutane	1-Butyne	Vinylacetylene	*n*-Butane	1-Butene
S_{ij}	3.55	3.25	11.7	0.191	0.115	12.7	3.20
S_{ij}^{IL}	3.67	3.34	12.5	0.193	0.117	13.5	3.30
Increase (%)[a]	3.21	2.52	7.11	1.21	1.74	6.64	3.03

[a] Increase (%) = $[(S_{ij}^{IL} - S_{ij})/S_{ij}] \times 100$.

Table 6 Group parameters of volume R and surface area Q

	CH_3CN^a	H_2O^a	$CH_2{=}CH^a$	$CH_2{}^a$	$CH_3{}^a$	$CH{=}CH^a$	CH^a	$CH{\equiv}C^a$	$[MMIM][PF_6]^b$
R	1.870	0.9200	1.345	0.6744	0.9011	1.117	0.4469	1.292	6.890
Q	1.724	1.400	1.176	0.5400	0.8480	0.8670	0.2280	1.088	6.044

[a] Parameters taken from the database in Aspen Plus. [b] Parameters derived from the corresponding basic groups.

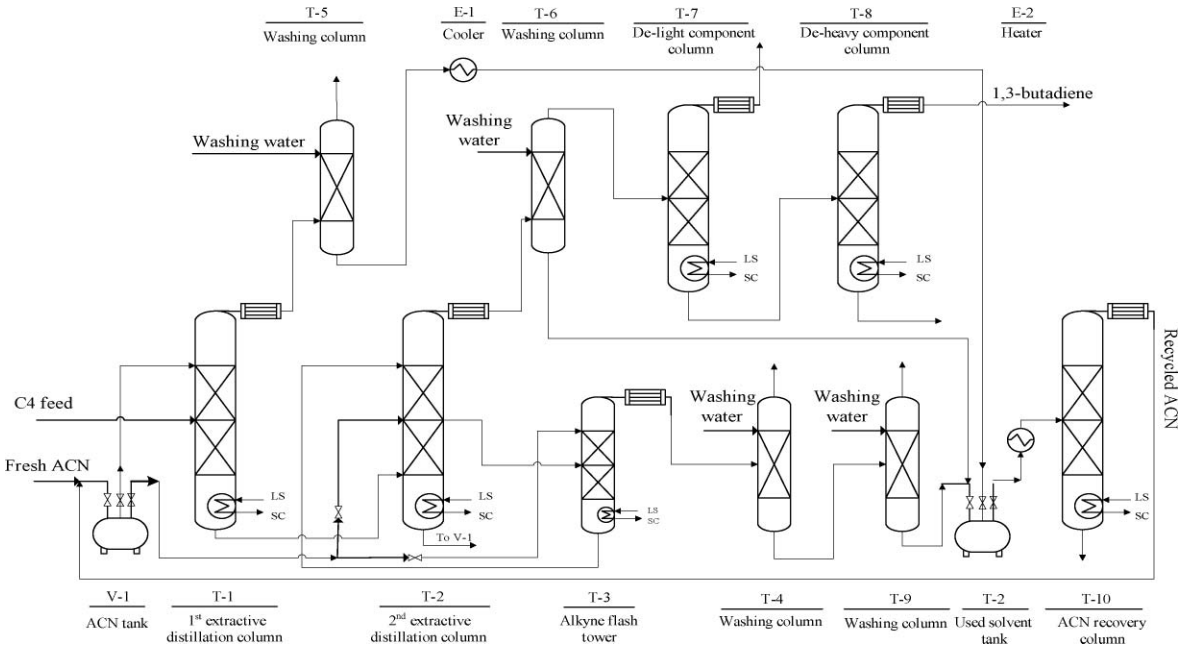

Fig. 15 Flowchart for a commercial ACN process to produce 1,3-butadiene.

$$\pi_1 = \sum_{k=1}^{n} \left\{ \left[\frac{\left(T_k^{\text{calc}} - T_k^{\text{COSMO}} \right)}{\sigma_T} \right]^2 + \left[\frac{\left(\gamma_{1,k}^{\text{calc}} - \gamma_{1,k}^{\text{COSMO}} \right)}{\sigma_{\gamma_1}} \right] \right\} \quad (5)$$

where T_k^{COSMO} and $\gamma_{1,k}^{\text{COSMO}}$ are the temperature and activity coefficient from the COSMO calculation, while σ_T and σ_{γ_1} are standard deviations, which were taken to be 0.18 K and 0.01. The superscript 'calc' refers to the values calculated by using the cUNIFAC model. The general information of the data used is summarized in Table 7, which indicates that the original UNIFAC model can describe the IL-containing systems well. In Table 8, the new group interaction parameters and some available parameters for the other groups are listed.

3.3 Process simulation

Process simulation technology in chemical engineering is an effective tool to analyze the performance of a novel process.

Table 7 Summary for the data sets used and correlation results

	$[C_2MIM][PF_6]$
Number of molecule solutes	9
Number of data sets	27
Number of data points	243
Temperature range (K)	298.15–343.15
Average RMSD (γ^{∞})	5.406

Based on plant data, simulations of a commercial ACN process and the proposed IL-containing process were carried out. The commercial ACN process simulated consists of four sections, as shown in Fig. 15: two extractive distillation sections, one ordinary distillation section, and one solvent purification section. In the first extractive distillation, the light components (with higher relative volatility than 1,3-BD) are removed. In the second extraction distillation, the heavy components are removed. In the ordinary distillation, the crude 1,3-BD is further purified to generate the product by removing the remaining light and heavy components. In the last section, the purification and recovery of the solvent mixture is completed.

As a comparison, only an IL decanter and an IL recovery column are added to the IL process to account for the presence of ionic liquids, as shown in Fig. 16. To be specific, the used extractive solvent in V-2 is fed to the IL decanter, and mixed with dichloromethane (DCM) which is proven experimentally to be an effective extracting agent. 99% of the IL in the solvent mixture will enter the DCM phase, and then the IL-containing mixture is fed to the IL recovery distillation column, in which DCM (as the top product) is recycled into the IL decanter, and IL (as the bottom product) is returned to the IL tank.

Based on the plant data and the results from COSMO-RS, both processes were simulated under identical conditions. The results are listed in Table 9 and Table 10. It was found that in the IL process the bottom temperatures (T_B) of the extractive distillation columns are lowered by 3.5 °C and 2.7 °C, the

Table 8 The group interaction parameters α_{ij} for the UNIFAC model[a]

	CH_3CN	H_2O	CH_2=CH	CH_2	CH_3	CH=CH	CH	CH≡C	[MMIM][PF_6]
CH_3CN	0	242.8	−40.62	24.82	24.82	−40.62	24.82	−203.0	170.0
H_2O	112.6	0	496.1	300.0	300.0	496.1	300.0	0	−272.0
CH_2=CH	336.9	270.6	0	−35.36	−35.36	0	−35.36	31.14	−210.0
CH_2	597.0	1318	86.02	0	0	86.02	0	298.9	2450
CH_3	597.0	1318	86.02	0	0	86.02	0	298.9	2450
CH=CH	336.9	270.6	0	−35.36	−35.36	0	−35.36	31.14	−242.0
CH	597.0	1318	86.02	0	0	86.02	0	298.9	60300
CH≡C	329.1	0	41.38	−72.88	−72.88	41.38	−72.88	0	−236.0
[MMIM][PF_6]	303.0	1059	750.0	1053	−159.0	710.0	11400	−23.67	0

[a] All group interaction parameters except those of [MMIM][PF_6] are taken from the database in Aspen Plus.

Table 9 Comparison of the key indices in both the IL-containing process and the no-IL process

	T_B of 1st column (°C)	T_B of 2nd column (°C)	Recovery of 1,3-butadiene	Purity of 1,3-butadiene	ACN consumption
No-IL process	119.7	153.8	95.33	99.58	1
IL process	116.2	151.1	96.04	99.58	0.86

Table 10 Comparison of the energy consumption (in GJ h^{-1}) at each stage of both the IL-containing process and the no-IL process

	T-1	T-2	T-7	T-8	T-10	T-11	P-1	P-2	P-3	E-2
No-IL process	36.55	33.77	0.1600	17.60	8.870	0.000	0.000	0.007	0.002	3.208
IL process	34.71	33.21	0.3700	17.70	5.310	0.400	0.015	0.007	0.006	1.803

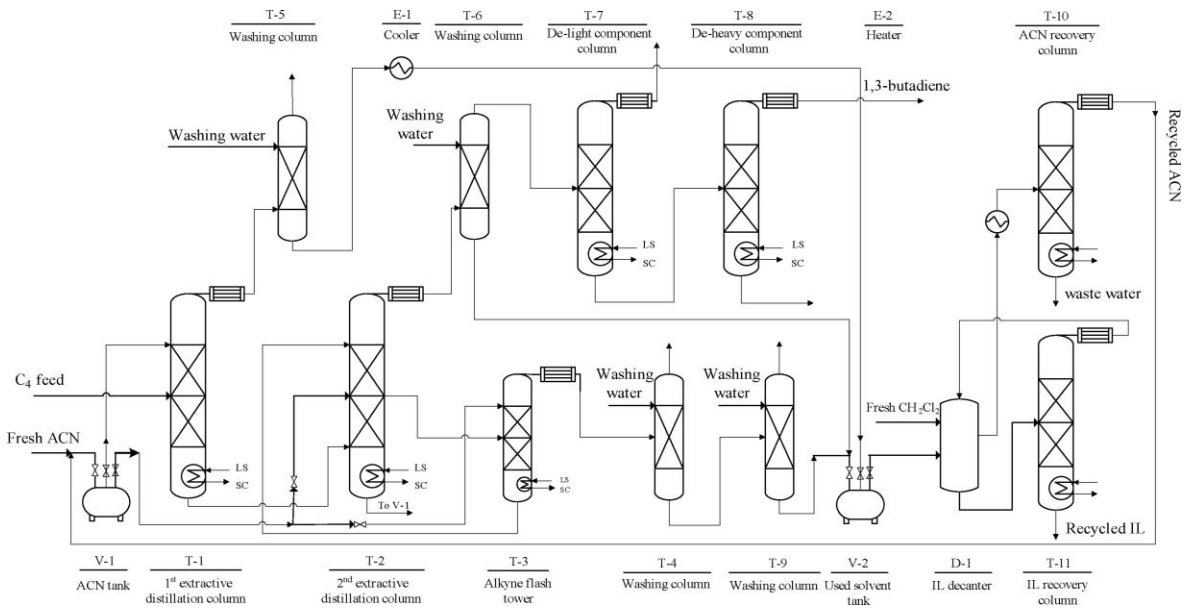

Fig. 16 Flowchart for the IL-containing ACN process to produce 1,3-butadiene.

recovery ratio of the product 1,3-BD is improved by 0.71%, the total energy consumption is reduced by 6.62%, and – most importantly – that the consumption of toxic ACN is decreased by 24%.

4. Conclusion

A multi-scale methodology has been developed for identifying a suitable ionic liquid for a new ACN process, integrating *ab initio* calculation, COSMOtherm calculation and process simulation. The *ab initio* calculation has enabled in-depth understanding of the interaction between ILs and C_4 fractions. It was found that the selectivity of the IL is mainly determined by its polarity, hydrogen-bonding ability with solutes, and molecular size. An IL with stronger polarity and hydrogen-bonding ability and smaller molecular size will possess a better selectivity. It was also found that the cation has limited influence on the ability of hydrogen bonding and only affects the polarity of ILs. It was concluded that the best ionic liquid for the separation of C_4 fractions is [C_2MIM][PF_6] derived from the results of the *ab initio* calculation. The prediction is in good agreement with experimental findings.

The COSMOtherm calculation revealed that the selectivity of the extractive solvent was improved by an average of 3.64% upon adding [C_2MIM][PF_6], confirming that the chosen ionic liquid is indeed efficient.

The process simulation indicates that, in the presence of [C_2MIM][PF_6] the temperatures at the bottoms of the extractive distillation columns are lowered by an average of 3.1 °C (which is significant enough to inhibit polymerization), that ACN consumption decreases by 24%, and that energy consumption decreases by about 6.62%.

In summary, this work has confirmed that the novel methodology developed in this study is a feasible and promising approach for identifying a suitable IL as an additive in current ACN processes. We shown how non-available thermodynamic data for a novel material are obtained based only on the molecular structure. Our method suggests a route to screen a suitable entrainer for a given separation process with different modeling techniques. It is not proposed as a replacement for experiment, but rather as a useful computer-aided tool for solvent and process design.

Abbreviations

k Group number.
P Pressure (kPa).
Q_k The surface parameters of group k.
R Gas constant (J mol^{-1} K^{-1}).
R_k The volume parameters of group k.
S Selectivity.
T Temperature (K).
V Molar volume.
x_i Mole fraction of component i in the liquid phase.
α_{jk} The adjustable group interaction parameters of the UNIFAC model accounting for the difference of short-range interactions between group j–k and k–k
γ The activity coefficient of component i.
γ^{∞} The infinite dilution activity coefficient of component i.
Δ The difference between the length of HB and the sum of van der Waals radii of the related atom.
δ Hansen's solubility parameter.
ξ The indication energy per unit volume.
π_1 Objective function.
σ Standard deviation.
Ψ Wavefunction.

Acknowledgements

The authors acknowledge the financial support provided by National Science Fund of China for Distinguished Young Scholar (No. 20625618), the Knowledge Innovation Program of the Chinese Academy of Sciences (KGCX2-YW-321), the National Key Technology R&D Program (2008BAF33B04), the National Basic Research Program of China (973 Program, No. 2009CB219901), and the Knowledge Innovation Program of the Institute of Process Engineering, Chinese Academy of Sciences (No. 082702).

References

1 M. M. Ammenheuser, W. E. Bechtold, S. Z. Abdel-Rahman, J. I. Rosenblatt, D. A. Hastings-Smith and J. B. Ward, *Environ. Health Perspect.*, 2001, **109**, 1249–1255.
2 N. Barshteyn, R. J. Krause and A. A. Elfarra, *Chem.-Biol. Interact.*, 2007, **166**, 176–181.
3 X. Y. Zhang and A. A. Elfarra, *Chem. Res. Toxicol.*, 2005, **18**, 1316–1323.
4 *US Pat.* 4401505, 1978.
5 *US Pat.* 4504692, 1985.
6 *US Pat.* 4128457, 1978.
7 X. J. Yang, X. Yin and P. K. Ouyang, *Chin. J. Chem. Eng.*, 2009, **17**, 27–35.
8 Z. G. Lei, H. Y. Wang, R. Q. Zhou and Z. T. Duan, *Comput. Chem. Eng.*, 2002, **26**, 1213–1221.
9 Y. Asano, K. Fujishiro, Y. Tani and H. Yamada, *Agric. Biol. Chem.*, 1982, **46**, 1165–1174.
10 Y. Asano, M. Tachibana, Y. Tani and H. Yamada, *Agric. Biol. Chem.*, 1982, **46**, 1175–1181.
11 M. J. Digeronimo and A. D. Antoine, *Appl. Environ. Microbiol.*, 1976, **31**, 900–906.
12 *Jpn Pat.* 57-105022, 1983.
13 D. Hongxing, L. Jian and P. Jian, *Chem. Ind. Time*, 2004, **18**, 16–19.
14 *Ger. Pat.*, 10114734, 2001.
15 H. S. Schrekker, M. P. Stracke, C. M. L. Schrekker and J. Dupont, *Ind. Eng. Chem. Res.*, 2007, **46**, 7389–7392.
16 M. H. Abraham, A. M. Zissimos, J. G. Huddleston, H. D. Willauer, R. D. Rogers and W. E. Acree, *Ind. Eng. Chem. Res.*, 2003, **42**, 413–418.
17 Z. B. Alfassi, R. E. Huie, B. L. Milman and P. Neta, *Anal. Bioanal. Chem.*, 2003, **377**, 159–164.
18 J. L. Anthony, E. J. Maginn and J. F. Brennecke, *J. Phys. Chem. B*, 2001, **105**, 10942–10949.
19 P. Wasserscheid and T. Welton, *Ionic Liquids in Synthesis*, Wiley-VCH, Weinheim, Germany, 2002.
20 D. Astruc, F. Lu and J. R. Aranzaes, *Angew. Chem., Int. Ed.*, 2005, **44**, 7852–7872.
21 J. E. Bara, C. J. Gabriel, S. Lessmann, T. K. Carlisle, A. Finotello, D. L. Gin and R. D. Noble, *Ind. Eng. Chem. Res.*, 2007, **46**, 5380–5386.
22 G. R. Yu, S. J. Zhang, G. H. Zhou, X. M. Liu and X. C. Chen, *AIChE J.*, 2007, **53**, 3210–3221.
23 A. Klamt and F. Eckert, *Fluid Phase Equilib.*, 2000, **172**, 43–72.
24 X. Hao, M. E. Djatmiko, Y. Y. Xu, Y. N. Wang, J. Chang and Y. W. Li, *Chem. Eng. Technol.*, 2008, **31**, 188–196.
25 W. F. Hou, H. Y. Su, Y. Y. Hu and J. Chu, *Chin. J. Chem. Eng.*, 2006, **14**, 584–591.
26 M. B. Nikoo and N. Mahinpey, *Biomass Bioenergy*, 2008, **32**, 1245–1254.
27 B. L. Yang, J. Wu, G. S. Zhao, H. J. Wang and S. Q. Lu, *Chin. J. Chem. Eng.*, 2006, **14**, 301–308.
28 M. J. Frisch, G. W. Trucks, H. B. Schlegel, G. E. Scuseria, M. A. Robb, J. R. Cheeseman, J. A. Montgomery, Jr., T. Vreven, K. N. Kudin, J. C. Burant, J. M. Millam, S. S. Iyengar, J. Tomasi, V. Barone, B. Mennucci, M. Cossi, G. Scalmani, N. Rega, G. A. Petersson, H. Nakatsuji, M. Hada, M. Ehara, K. Toyota, R. Fukuda, J. Hasegawa, M. Ishida, T. Nakajima, Y. Honda, O. Kitao, H. Nakai, M. Klene, X. Li, J. E. Knox, H. P. Hratchian, J. B. Cross, V. Bakken, C. Adamo, J. Jaramillo, R. Gomperts, R. E. Stratmann, O. Yazyev, A. J. Austin, R. Cammi, C. Pomelli, J. Ochterski, P. Y. Ayala, K. Morokuma, G. A. Voth, P. Salvador, J. J. Dannenberg, V. G. Zakrzewski, S. Dapprich, A. D. Daniels, M. C. Strain, O. Farkas, D. K. Malick, A. D. Rabuck, K. Raghavachari, J. B. Foresman, J. V. Ortiz, Q. Cui, A. G. Baboul, S. Clifford, J. Cioslowski, B. B. Stefanov, G. Liu, A. Liashenko, P. Piskorz, I. Komaromi, R. L. Martin, D. J. Fox, T. Keith, M. A. Al-Laham, C. Y. Peng, A. Nanayakkara, M. Challacombe, P. M. W. Gill, B. G. Johnson, W. Chen, M. W. Wong, C. Gonzalez and J. A. Pople, *GAUSSIAN 03 (Revision C.02)*, Gaussian, Inc., Wallingford, CT, 2004.
29 A. D. Becke, *J. Chem. Phys.*, 1993, **98**, 5648–5652.
30 C. T. Lee, W. T. Yang and R. G. Parr, *Phys. Rev. B: Condens. Matter*, 1988, **37**, 785–789.
31 A. Klamt and F. Eckert, *Abstr. Pap. Am. Chem. Soc.*, 2000, **220**, 234.
32 A. Klamt and F. Eckert, *Fluid Phase Equilib.*, 2004, **217**, 53–57.
33 A. Klamt and F. Eckert, *Fluid Phase Equilib.*, 2007, **260**, 183–189.
34 R. Ahlrichs, M. Bar, M. Haser, H. Horn and C. Kolmel, *Chem. Phys. Lett.*, 1989, **162**, 165–169.
35 O. Treutler and R. Ahlrichs, *J. Chem. Phys.*, 1995, **102**, 346–354.

36 J. M. Prausnitz and R. Anderson, *AIChE J.*, 1961, **7**, 96–101.
37 *US Pat.* 2371908, 1940.
38 M. H. Abraham and W. E. Acree, *Green Chem.*, 2006, **8**, 906–915.
39 J. Cheng, P. Hu, P. Ellis, S. French, G. Kelly and C. M. Lok, *J. Phys. Chem. C*, 2009, **113**, 8858–8863.
40 L. Fang, H. Zhang, W. Cui and M. J. Ji, *J. Chem. Inf. Model.*, 2008, **48**, 2030–2041.
41 Y. Hayashiuchi, T. Hagihara and T. Okada, *Physica B+C*, 1982, **115**, 67–71.
42 P. Pawlow, *Z. Phys. Chem.*, 1909, **65**, 545–548.
43 E. Schrader and H. G. Zachmann, *Kolloid. Z. Z. Polym.*, 1970, **241**, 1015–1025.
44 C. Q. Sun, Y. Wang, B. K. Tay, S. Li, H. Huang and Y. B. Zhang, *J. Phys. Chem. B*, 2002, **106**, 10701–10705.
45 K. Dong, S. J. Zhang, D. X. Wang and X. Q. Yao, *J. Phys. Chem. A*, 2006, **110**, 9775–9782.
46 A. Bagno, F. D'Amico and G. Saielli, *ChemPhysChem*, 2007, **8**, 873–881.
47 R. C. Remsing, J. L. Wildin, A. L. Rapp and G. Moyna, *J. Phys. Chem. B*, 2007, **111**, 11619–11621.
48 G. R. Yu, S. J. Zhang, X. Q. Yao, J. M. Zhang, K. Dong, W. B. Dai and R. Mori, *Ind. Eng. Chem. Res.*, 2006, **45**, 2875–2880.
49 X. L. Yuan, S. J. Zhang, J. Liu and X. M. Lu, in *4th International Symposium on Molecular Thermodynamics and Molecular Simulation*, Makuhari, Japan, 2006, pp. 195–200.
50 *Jpn Pat.* 53-111001, 1978.
51 Z. G. Lei, W. Arlt and P. Wasserscheid, *Fluid Phase Equilib.*, 2006, **241**, 290–299.
52 C. Jork, C. Kristen, D. Pieraccini, A. Stark, C. Chiappe, Y. A. Beste and W. Arlt, *J. Chem. Thermodyn.*, 2005, **37**, 537–558.
53 J. F. Wang, W. Sun, C. X. Li and Z. H. Wang, *Fluid Phase Equilib.*, 2008, **264**, 235–241.
54 A. Fredenslund, R. L. Jones and J. M. Prausnitz, *AIChE J.*, 1975, **21**, 1086–1099.
55 A. Bondi, *Physical Properties of Molecular Crystals, Liquids and Glasses*, John Wiley & Sons, New York, 1968.